Gradstein, F. M., Ludden, J. N., et al., 1992
Proceedings of the Ocean Drilling Program, Scientific Results, Vol. 123

35. GEOCHEMICAL WELL LOGS FROM THE ARGO ABYSSAL PLAIN AND EXMOUTH PLATEAU, NORTHEAST INDIAN OCEAN, SITES 765 AND 766 OF LEG 123[1]

Elizabeth Lewis Pratson,[2] Cristina Broglia,[2] and David Castillo[3]

ABSTRACT

Geochemical well logs were obtained in sediments at Site 765 and in both sediments and basalts at Site 766 of Leg 123. Corrections have been applied to the logs to account for variations in hole size, drilling fluid interference, and casing or drill pipe attenuation. Weight fractions of the major oxides and of calcium carbonate have been calculated from the reprocessed logs, and the results correlate well with shipboard $CaCO_3$ and X-ray fluorescence measurements. The logs show good qualitative agreement with the overall lithologic trends of Hole 765D and excellent qualitative agreement with cores from Hole 766A.

INTRODUCTION

Leg 123 was combined with Leg 122 to continue a transect of drill sites in the northeast Indian Ocean across the northwestern coast of Australia. Drilling during Leg 122 established the central portion of this transect and concentrated on the post-Permian sediments of the Exmouth Plateau. During Leg 123, drilling extended the transect from the Argo Abyssal Plain (Site 765) in the northeast into the Exmouth Plateau escarpment (Site 766) in the southwest. The primary objective of this leg was to study the continental/oceanic basement and early oceanic sediments on this passive margin (Shipboard Scientific Party, 1990a, 1990b).

Both sites drilled during Leg 123 (Sites 765 and 766) were logged with a complete set of tools, including a geochemical tool string. Geochemical log measurements are used to derive the weight fractions of the major oxides present in the formation at intervals of 0.1524 m. This chapter describes the hole conditions and logging operations at each site, presents the basic principles and modes of operation of the geochemical tools, explains the data processing techniques, and compares the final natural gamma-ray and oxide/calcium carbonate fractions estimated from the logs to discrete core measurements.

GEOCHEMICAL TOOL STRING

The geochemical logging tool string (GLT) consists of four logging tools: the natural gamma-ray tool (NGT), the compensated neutron tool (CNT), the aluminum activation clay tool (AACT), and the gamma-ray spectrometry tool (GST) (GLT, NGT, CNT, AACT, and GST are trademarks of Schlumberger Inc.; Fig. 1). The NGT is located at the top of the tool string, so that it can measure the naturally occurring radionuclides, thorium (Th), uranium (U), and potassium (K), before the formation is irradiated by the nuclear sources contained in the other tools. The CNT, located below the NGT, carries low-energy californium-252 (^{252}Cf) to activate the aluminum (Al) atoms in the formation. The AACT, a modified NGT, is located below the ^{252}Cf source and measures the activated gamma rays in the formation. By combining the ACT measurement with the previous NGT measurement, background radiation can be subtracted out and a reading of formation Al can be obtained (Scott and Smith, 1973). The GST, at the base of the string, carries a pulsed neutron generator to bombard the borehole and formation and an NaI(Tl) scintillation detector, which measures the spectrum of gamma rays generated by neutron-capture reactions. Because each of the elements in the formation is characterized by a unique spectral signature, it is possible to derive the contribution (or yield) of each of the major elements, silicon (Si), iron (Fe), calcium (Ca), titanium (Ti), sulfur (S), gadolinium (Gd), and potassium (K), to the measured spectrum and, in turn, to estimate its abundance in the formation. The GST also measures the hydrogen (H) and chlorine (Cl) in the borehole and formation, but these elements are not used for determining rock geochemistry.

The only major rock-forming elements not measured by the GLT are magnesium (Mg) and sodium (Na); the neutron-capture cross sections of these elements are too small relative to their typical abundances for the tool string to detect them. One can estimate the approximate Mg + Na values by using the photoelectric factor (PEF), measured by the lithodensity tool (LDT). This measured PEF can be compared with a calculation of PEF from all of the measured elements. In theory, the separation between the measured and calculated PEF is attributable to any element left over in the formation (i.e., Mg and Na). Further explanation of this technique can be found in Hertzog et al. (1987). We did not perform this calculation for either Hole 765D or Hole 766A, because the PEF measurement was affected in both holes (1) by the presence of barite in the mud, (2) by previous activation from the GLT, and (3) by attenuation caused by pipe and/or casing.

DATA ACQUISITION

Because of unstable hole conditions and time constraints, most of the logging data used in our processing was obtained through pipe or casing. Electrical and acoustical logs do not work through pipe, as neither electrical currents nor sound waves propagate through steel. On the other hand, neutrons and gamma rays can pass and be detected through pipe or casing; thus, geochemical and radioactive logs can be recorded in this manner. However, the signal detected from the formation is greatly attenuated and decreases the signal-to-noise ratio. The basement section at Hole 765D was logged open hole and provided the highest quality geochemical data obtained during Leg 123.

Site 765

Of the four holes drilled at Site 765, only Holes 765C and 765D were logged. The original plan was to log open hole the upper section of sediments in Hole 765C, and then to case the sediment

[1] Gradstein, F. M., Ludden, J. N., et al., 1992. *Proc. ODP, Sci. Results,* 123: College Station, TX (Ocean Drilling Program).
[2] Borehole Research Group, Lamont-Doherty Geological Observatory of Columbia University, Palisades, NY 10964, U.S.A.
[3] Dept. of Geophysics, Stanford University, Stanford, CA 94305, U.S.A.

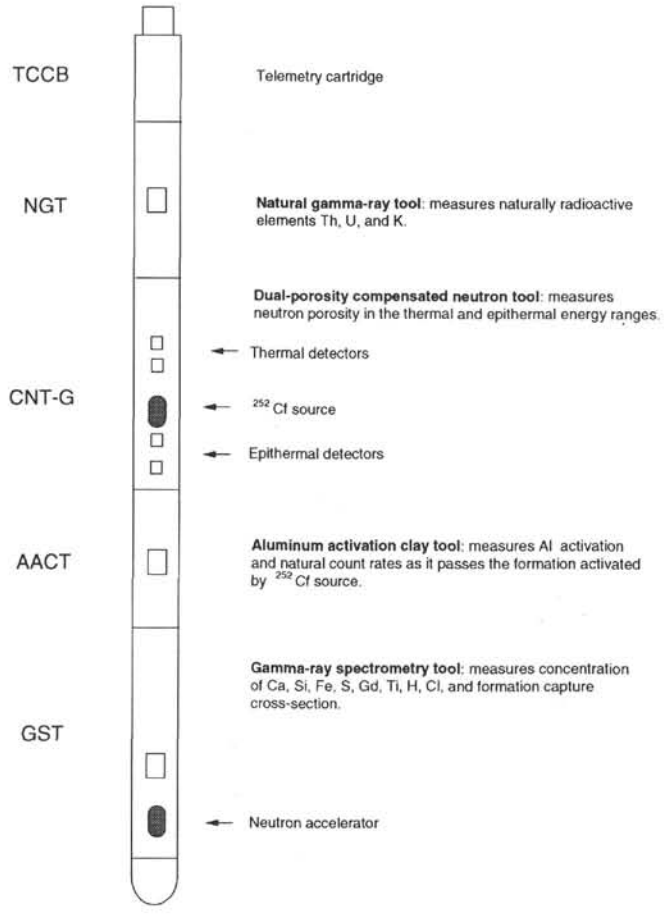

Figure 1. Schematic drawing of the GLT used by ODP. The tool has since been modified for ODP to include a boron sleeve, which masks out Fe readings from the tool itself.

section in the adjacent Hole 765D, so that the basement section could be logged open hole. Hole 765C was drilled to 949 m below sea floor (mbsf), and then three slugs of mud were circulated in preparation for logging. This mud contained 0.3% heavyweight barite (to remove cavings at the bottom of the hole during circulation) and 5% KCl (to stabilize swelling of clays). Adverse hole conditions at Hole 765C, including a 4° to 10° deviation of the hole and differential pressure between the heavy muds in the formation and the less heavy fluids in the drill hole, prevented Leg 123 scientists from recording the entire suite of logging data planned for this hole. The seismic stratigraphic string (acoustic, resistivity, and gamma-ray tools) recorded data open hole from 652 to 184 mbsf, with a through-pipe interval from 421 to 525 mbsf. The LDT was then run open hole from 475 to 156 mbsf. Because of time constraints, the shipboard scientists decided not to run the GLT open hole in Hole 765C, but instead to run it in adjacent Hole 765D.

Hole 765D was spudded approximately 30 m from Hole 765C. The hole was drilled to 948 mbsf (12 m below the sediment/basalt interface), where casing was set and latched into a reentry cone. Cement was pumped between the casing and drill hole wall. The hole was then cored to 1194 mbsf, 258 m into basement. Three logging runs were completed at this hole: one with the seismic stratigraphic tool string (SS), another with the GLT, and the third with the LDT. The SS logs were recorded open hole from 1180 to 933 mbsf, through casing from 933 to 55 mbsf, and through casing and pipe in the upper 55 mbsf. The GLT was run from 1165.8 to 933 mbsf open hole and from 933 to 169 mbsf through casing. The upper 169 m was not logged, because the tool stuck in the casing. Pipe was then lowered through casing to 870 mbsf to prevent any further sticking when recording the LDT logs. Because this string was run through both pipe and casing after the formation had been activated by the nuclear sources of the GLT, the readings can be considered valid only from a qualitative point of view.

Site 766

Drilling at Hole 766A reached a total depth of 527.2 mbsf, with 58.4 m in basement. Prior to the three logging runs, the hole had been conditioned and filled with barite (52 ppb) and KCl (4%) mud. Pipe was raised to 260 mbsf, and SS logs were recorded open hole from 443 to 260 mbsf and through pipe from 260 mbsf to the seafloor. Because a bridge occurred at 443 mbsf, no logging could be conducted in the lower part of the hole. To clear this obstruction and to ensure a complete pass of the geochemical logs through the basement section of the well, pipe was run to the bottom of the hole. The GLT then was run through pipe from 527 mbsf to the seafloor. Next, the LDT was run. Pipe was pulled up to 245 mbsf, where a bridge at 442 mbsf again prevented openhole logging into basement. As with the data from Hole 765D, those from Hole 766A were recorded after the geochemical run and thus were affected by formation activation from the ^{252}Cf source.

DATA REDUCTION

Well log data from the Schlumberger tools are transmitted digitally up a wireline and are recorded and processed on board the *JOIDES Resolution* in the Schlumberger Cyber Service Unit (CSU). Results from the CSU are made available as "field logs" for initial shipboard interpretation. Subsequent reprocessing is necessary to correct data for the effects of fluids added to the well, for logging speed, and for pipe interference. Processing of the spectrometry data is required to transform the relative elemental yields into oxide weight fractions.

Processing is performed with a set of log interpretation programs written by Schlumberger. The steps are summarized in the next sections.

Reconstruction of Relative Elemental Yields from Recorded Spectral Data

The first processing step uses a weighted, least-squares method to compare the measured spectra from the GST with a series of standard spectra to determine the relative contribution (or yield) of each element. Whereas six elemental standards (Si, Fe, Ca, S, Cl, and H) are used to produce the shipboard yields, three additional standards (Ti, Gd, and K) can be used in shore-based processing to improve the spectra (Grau and Schweitzer, 1989). Although these additional elements often appear in the formation in low concentrations, they can contribute greatly to the measured spectra because they have large neutron-capture cross sections. For example, the capture cross section of Gd is 49,000 barns; that of Si is 0.16 barns (Hertzog et al., 1987). Although occurring in small abundances in the formation, Gd is included in the calculation of a best fit between the measured and standard spectra. This best-fit analysis was performed for the elements in each of the holes logged during Leg 123 and included spectral standards for Si, Ca, Fe, Ti, Gd, S, H, Cl, and K.

Before the yields can be manipulated further, the Fe yield has to be corrected for the Fe contained in (1) the steel drill pipe, (2) the bottom hole assembly, (3) the casing, and (4) the tool itself. Although a boron sleeve is routinely used by Schlumberger, one cannot use it yet in ODP drill holes because the diameter of the drill pipe through which the tool must pass is too small. The detector thus picks up Fe from the tool itself. After corrections for

Fe were completed, a straight, 10-point, smoothing filter was applied to all the yields in both holes to reduce the amplitude of noise in the data.

Calculation of Total Radioactivity and Th, U, and K Concentrations

The second step in log processing uses the counts in five spectral windows from the NGT (Lock and Hoyer, 1971) to calculate the total radiation from natural gamma rays in the formation, as well as concentrations of Th, U, and K. This resembles the routine performed at sea, except that hole-size changes are corrected during shore-based processing of these curves.

Filtering of the natural gamma-ray logs is necessary to reduce statistical errors that often create erroneous negative readings and anti-correlations (especially between Th and U). A Kalman-type filter (Ruckebusch, 1983) is applied at sea to reduce these effects. An alpha filter, which heavily smooths the five measured energy channels while holding the total gamma-ray value constant (C. Flaum, pers. comm., 1989), was applied when processing data from Hole 765D. A slightly more sophisticated Kalman filter was applied during shore-based processing of Hole 766A data. At each depth level, calculations and corrections also were performed for any K contained in the mud. This correction for K is particularly useful when processing data gathered from ODP holes, where KCl is added routinely; however, because of its dispersion it is difficult to know exactly how much K actually is in the borehole. The data output from this program include values for K (wet wt%), U (ppm), and Th (ppm), along with a total gamma-ray curve and a computed gamma-ray curve (total gamma ray minus U contribution).

Calculation of Al Concentration

The third processing routine is used to calculate an Al curve using four energy windows, while correcting concurrently for natural activity, borehole fluid neutron-capture cross section, formation neutron-capture cross section, formation slowing-down length, and borehole size. Porosity and density logs are necessary for converting the wet weight percent K and Al curves to dry weight percent. Porosity and density curves were obtained from the LDT. Log data had to be rescaled to agree with core values, because the ^{252}Cf in the GLT activated the casing and formation. Interpolated density and porosity core measurements were spliced onto these logs at Hole 766A, where no density or porosity log data were available.

We also corrected for Si interference with Al; the ^{252}Cf source activates the Si, producing the aluminum isotope, ^{28}Al (Hertzog et al., 1987). The program uses the Si yield from the GST to determine the Si background correction. The program outputs dry weight percentages of Al and K, which are used for calculating and normalizing the remaining elements.

Normalization of Elemental Yields from the GST to Calculate the Elemental Weight Fractions

The next routine combines the dry weight percentages of Al and K with the reconstructed yields to obtain dry weight percentages of the GST elements using the relationship:

$$Wt_i = FY_i/S_i, \quad (1)$$

where Wt_i = absolute elemental concentration, F = normalization factor, Y_i = relative elemental yield, and S_i = tool spectral sensitivity. The normalization factor, F, is a calibration factor determined at each depth from a closure argument to account for the number of neutrons captured by a specific concentration of rock elements. Because the sum of oxides in a rock is 100%, F is given by

$$F\,(\Sigma_i X_i Y_i/S_i) + X_K Wt_K + X_{Al} Wt_{Al} = 100, \quad (2)$$

where X_i = dry wt% of oxide or carbonate ÷ dry wt% of element i, Y_i = fraction of spectra attributed to element i, S_i = sensitivity factor, X_K = dry wt% of oxide of element K ÷ dry wt% of K, Wt_K = dry wt% K, X_{Al} = dry wt% of oxide of element Al ÷ dry wt% of Al, and Wt_{Al} = dry wt% Al. The sensitivity factor, S_i, is a tool constant measured in the laboratory that depends on the capture cross section, gamma-ray production, and detection probabilities of each element measured by the GST (Hertzog et al., 1987).

The value X_i accounts for the C and O associated with each element. Table 1 lists the oxide factors used in this calculation. All of the measured elements associate with C and O in a constant ratio, except for Ca, which associates with C and O in one of two ways: $CaCO_3$ or CaO. To convert the measured yields to elements/oxides, the dominant form of Ca must be assumed. The assumption is made based on the lithologic description of the cores. In both Holes 765D and 766A, the oxide factor for $CaCO_3$ was used throughout the sedimentary section, and CaO was used throughout the basement section.

Calculation of Oxide Percentages

The fifth and final routine simply multiplies the percentage of each element by its associated oxide factor with the same oxide factors as were used in the previous step (Table 1).

COMPARISON OF GEOCHEMICAL LOGS TO CORE

Site 765 (Sediment Section)

The processed natural gamma-ray curves from Hole 765C are shown in Figure 2. Reprocessing improved the initial field logs, in which the K value was negative from an overcorrection for KCl. To maximize openhole data, the logs presented have been spliced from different logging passes. The interval from 156 to 475 mbsf contains spectral logs from the openhole LDT logging pass; the interval from 475 to 525 mbsf contains spectral logs from the SS logging run, corrected for pipe attenuation; and the interval from 525 to 634 mbsf contains openhole spectral data from the SS. The results indicate a general increase in clay content with depth, which coincides with lithologic descriptions of the core (Shipboard Scientific Party, 1990a).

The boundary between Unit II and Unit III is marked by a large increase in Th content and slight increase in K content. Subunit IIIB is differentiated from Subunit IIIA by a sharp increase in K content. Unit IV is identified on the spectral logs as an additional increase in K and Th.

The cased-hole sediment section of Hole 765D was processed separately from the openhole basalt section. The processed natural gamma-ray logs from the sediment section of the well presented here come from the GLT (Fig. 3). Although these logs were

Table 1. Oxide factors used when normalizing elements to 100% and converting elements to oxides.

Element	Oxide/carbonate	Conversion factor
Si	SiO_2	2.139
Ca	$CaCO_3$	2.497
	CaO	1.399
Fe	FeO*(total iron)	1.358
K	K_2O	1.205
Ti	TiO_2	1.668
Al	Al_2O_3	1.658
Mg	MgO	1.658

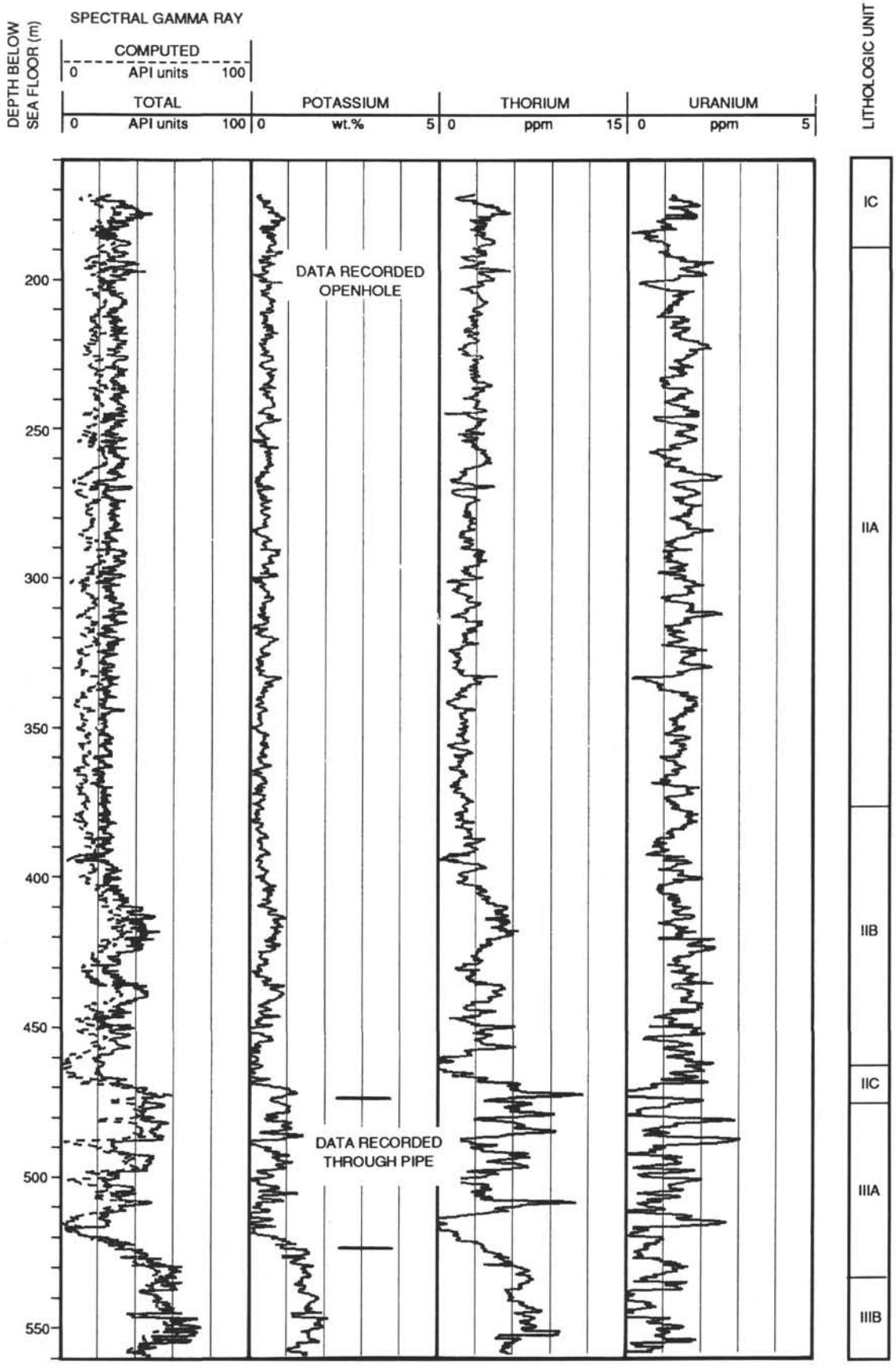

Figure 2. Processed natural gamma-ray curves from Hole 765C.

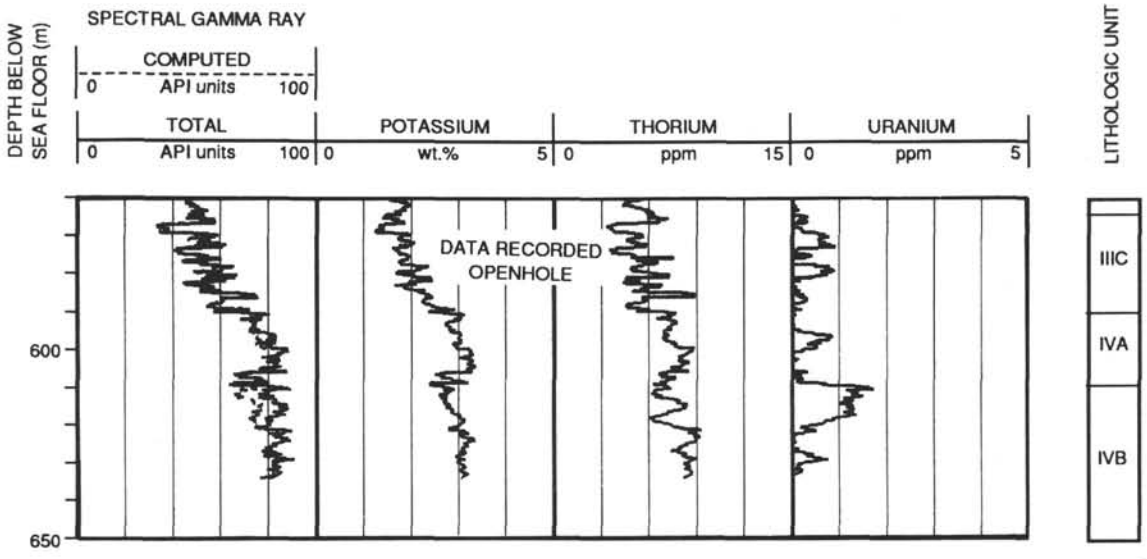

HOLE 765-C: LEGEND OF LITHOLOGIC UNITS

Subunit IA: redeposited clayey calcareous sediments and clayey siliceous ooze
Subunit IB: clayey calcareous sediments, conglomerates, and turbidites
Subunit IC: clayey calcareous sediments and silty clay
Subunit IIA: redeposited calcareous sediments
Subunit IIB: redeposited calcareous sediments and clay
Subunit IIC: redeposited calcareous sediments overlying conglomerate
Subunit IIIA: calcareous sediments and clay
Subunit IIIB: calcareous sediments, conglomerate, and claystone
Subunit IIIC: clayey chalk, claystone, and black shale
Subunit IVA: zeolitic clay and calcareous sediments
Subunit IVB: claysand calcareous sediments
Subunit IVC: claystone and clacareous sediments
Subunit IVD: mixed-redeposited sediments
Subunit VA: claystonesand silty layers
Subunit VB: claystone
Subunit VC: claystone and radiolarite
Unit VI: chalks and claystone
Subunit VIIA: claystones and radiolarite
Subunit VIIB: claystone

Figure 2 (continued).

recorded through casing, the results are comparable to openhole logs from Hole 765C.

In Figure 4, we compare the K curves from the two holes with a log of interpolated K core data from Holes 765B and 765C. The K values from logs and cores at Hole 765C have been corrected for a hole deviation of from 4° to 10°. Hole deviation must be accounted for when comparing the two data sets, because the depth difference was as high as 8.8 m at the bottom of the well. The logs prove that the K-rich claystones of Unit IV are continuous over the 30 m between Holes 765C and 765D.

In Figure 5, we present the oxide weight fractions estimated from the logs in the sediment section of Hole 765D. These can be compared to the interpolated XRF measurements from Holes 765B and 765C (Fig. 6). Because of the low signal-to-noise ratio resulting both from the casing and from the high porosity of these sediments, the log results are considered qualitative, useful in distinguishing some major lithologic changes.

Three major zones can be distinguished based on the oxide log responses. The first zone (156–470 mbsf) is characterized by a slightly higher $CaCO_3$ content and by lower values of Al_2O_3 and K_2O. A slightly lower reading of SiO_2, along with an increase in signal-to-noise ratio, also is seen in this upper section of the well. The noise increase in this section probably was caused by high porosity, which generates less signal from the formation and more from Cl and H in the pore spaces.

The second zone (470–640 mbsf) is marked by an increase in K_2O and Al_2O_3, roughly correlating to the transition from more calcareous sediments of Unit III to the claystones of Unit IV (Fig. 6; Shipboard Scientific Party, 1990a).

The third zone (640–930 mbsf) is marked by a decrease in K_2O and Al_2O_3 and by a slight increase in SiO_2. This coincides with the core description of claystones in Units V, VI, and VII. Variations in Fe content in this zone agree with those in the core. Overall variations in Fe content also follow the trend of the K_2O

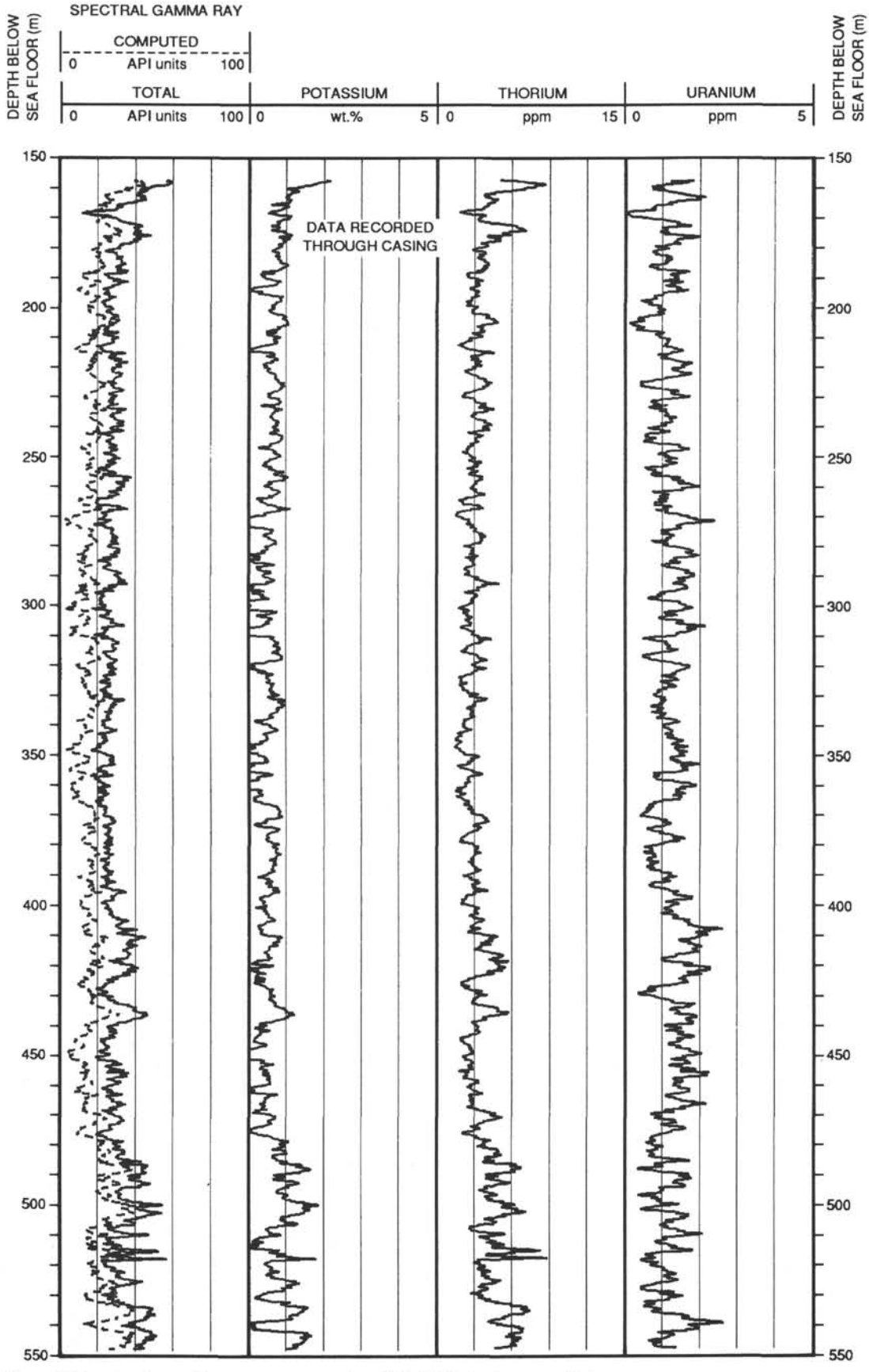

Figure 3. Processed natural gamma-ray curves from Hole 765D (sediment section).

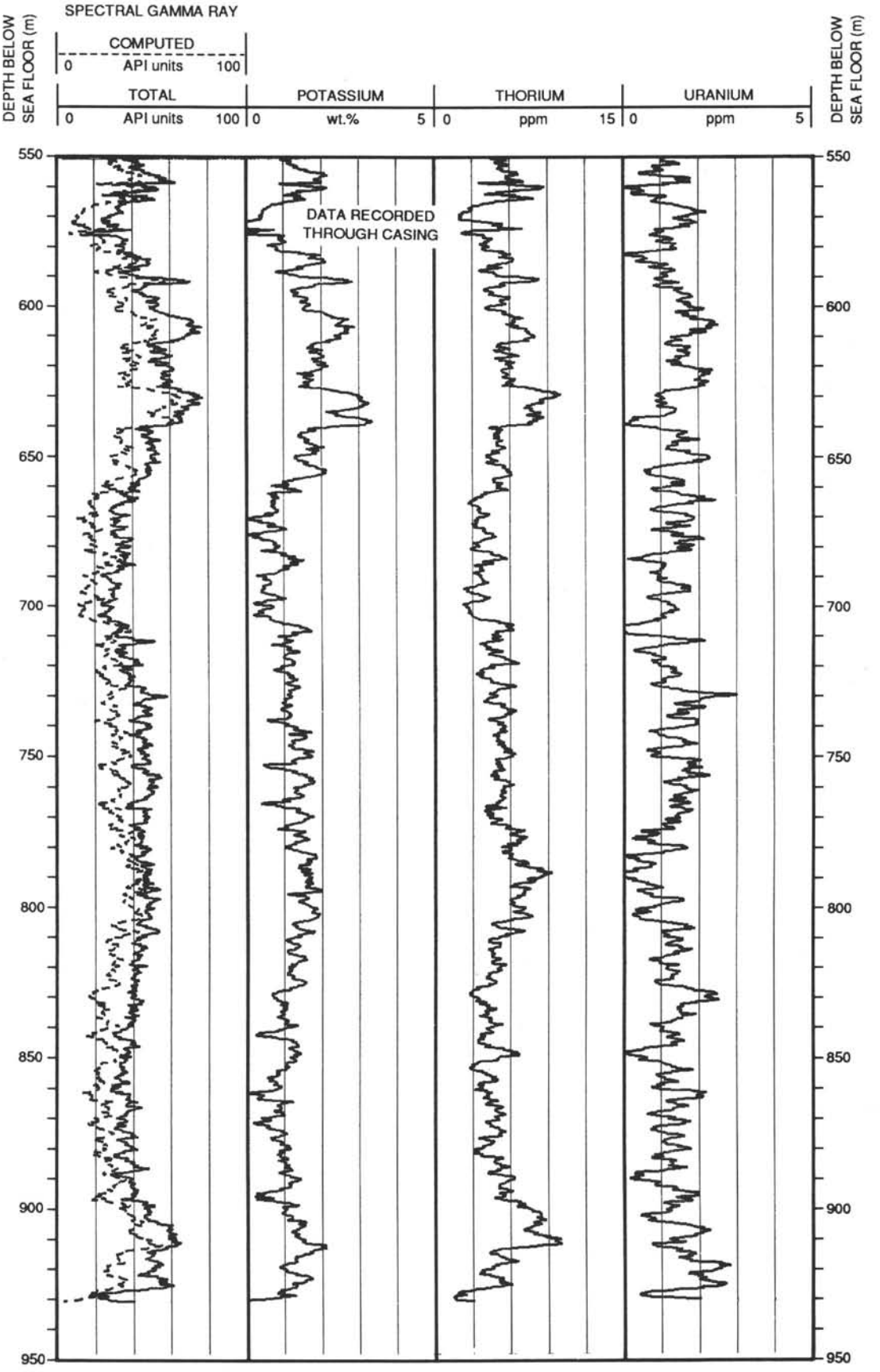

Figure 3 (continued).

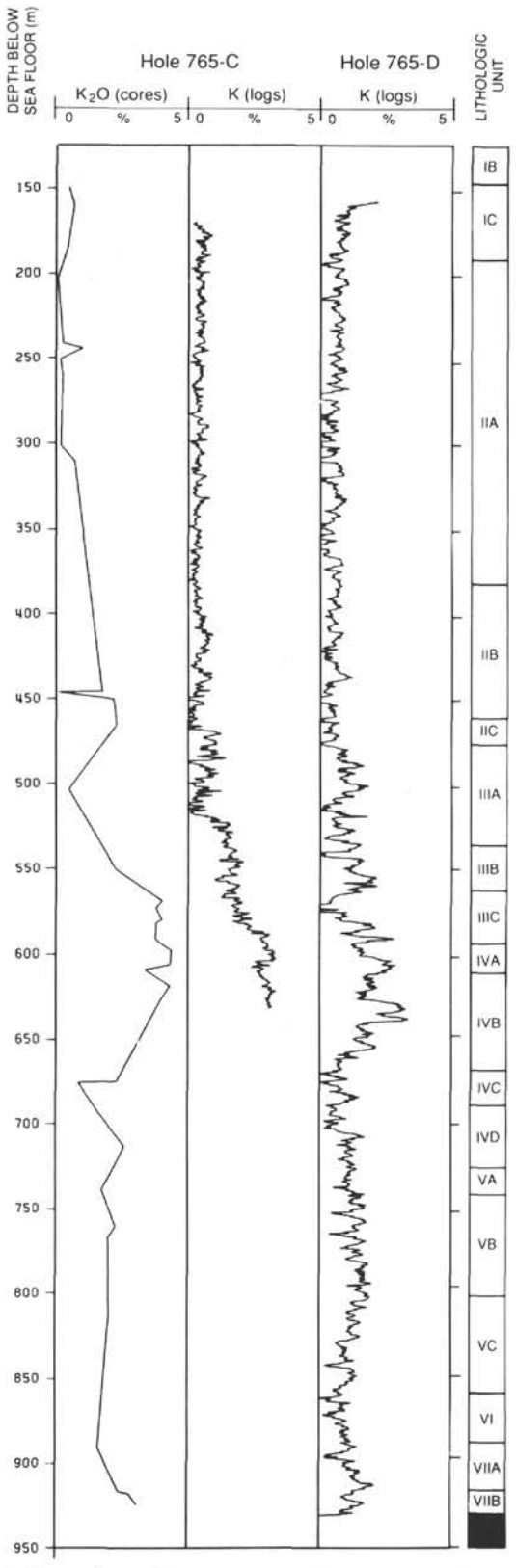

Figure 4. Comparison of K measurements from cores and logs at Holes 765C and 765D. K_2O and K expressed, respectively, as dry weight percent and wet weight percentages. Data from Hole 765C are corrected for hole deviation. Note the increase in K log response at about 450 mbsf, which corresponds to the increase in the clay fraction of the sediments observed in Hole 765C.

log, indicating that illite may be a dominant clay type (see clay XRF measurements, Shipboard Scientific Party, 1990a).

Site 765 has been termed a "geochemical reference section" (Shipboard Scientific Party, 1990a). One of the objectives of this section is to provide geochemical reference data for the composition of sediments and basement near oceanic trenches. This chemical data can be used when calculating global geochemical mass balances of the chemistry of arc volcanics. The geochemical well-log information provided by these logs helps to refine the vertical and horizontal extent of the lithologic units and provides measurements for calculating "bulk" geochemical compositions of these sediments.

Site 765 (Basement Section)

Geochemical data from the openhole basement section of the drill site was processed by Bruce Lyons at Schlumberger Well Service in New Orleans. The natural gamma-ray curves are presented in Figure 7.

In Figure 8, we show the oxide weight percentages and XRF measurements from cores. The scientific shipboard party defined 16 igneous rock units in the logged section of Hole 765D through lithological and geochemical variations (Shipboard Scientific Party, 1990a). These logs compare well with core measurements, especially those of Al_2O_3, Fe_2O_3, CaO, and K_2O. The SiO_2 estimates from the logs are higher than SiO_2 measurements from the cores, perhaps because MgO and Na_2O were not calculated in the logs. The log-derived TiO_2 also is slightly higher.

Site 766A

The processed natural gamma-ray logs from the GLT are presented in Figure 9. Drill-pipe attenuation and bottom-hole assembly (BHA) were corrected. The geochemical logs also were corrected to account for the Fe in the pipe and in the BHA. Final calculations of the oxides are presented in Figure 10.

The geochemical logs at this site agree well with the lithologic core descriptions (Shipboard Scientific Party, 1990b). A change in the geochemical logs at 15 mbsf roughly coincides with the change in lithology between Subunits IA and IB, recorded at 7 mbsf in the cores. This change is most clearly distinguished in the total gamma-ray and Al_2O_3 curves, which indicate slightly more clay in Subunit IA.

An increase in K and Th in the spectral logs and a decrease in $CaCO_3$ indicate the boundary between Units I and II. The claystones of Unit III are characterized by a sharp increase in K and Th and in SiO_2, Al_2O_3, and FeO* at the expense of $CaCO_3$. The low signal-to-noise ratio seen in the spectral logs from the bottom of the well (414 mbsf) was caused by the BHA. There, pipe diameter increased from 5 to 8.25 in., which greatly attenuated the signal. The sediment/basement contact is defined at 466 mbsf by an increase in the Al_2O_3 curve and a decrease in the SiO_2 curve. The K curve is high in the basement section, possibly the result of an overcorrection for attenuation.

CONCLUSIONS

Reprocessing of natural gamma-ray logs improves measurements obtained in the field by incorporating hole-size corrections and better calibrations of Th, U, and K, thus eliminating the negative values that occur in field logs. The K curve can be a useful tool for correlating between Holes 765C and 765D; well logs show that the K-rich claystones of Unit IV are continuous over the 30 m between the two holes. Geochemical logs can be converted to elemental and oxide measurements, which compare well with core measurements and lithologic descriptions. When core data are missing or sparse, the reprocessed logs represent an invaluable data set from which to interpret lithology. In particular, the $CaCO_3$ curve shows relative increases or decreases in carbon-

ate content in the sediments, and the Al_2O_3 and K_2O curves are excellent clay indicators.

ACKNOWLEDGMENT

The authors would like to acknowledge Bruce Lyons for all his effort in processing the data. We also thank Jennifer Tivy for reviewing the paper and for all her useful comments.

REFERENCES

Grau, J., and Schweitzer, J. S., 1989. Elemental concentrations from thermal neutron-capture gamma-ray spectra in geological formations. *Nucl. Geophys.*, 3(1):1–9.

Hertzog, R., Colson, L., Seeman, B., O'Brien M., Scott, H., McKeon, D., Grau, J., Ellis, D., Schweitzer, J., and Herron, M., 1987. *Geochemical Logging With Spectrometry Tools:* Dallas (Soc. Pet. Engrs.), Pap. 16792.

Lock, G. A., and Hoyer, W. A., 1971. Natural gamma-ray spectral logging. *The Log Analyst,* 12(5):3–9.

Ruckebusch, G., 1983. A Kalman filtering approach to natural gamma-ray spectroscopy in well logging. *Inst. Electr. Electron. Eng., Trans.,* AC-28(3):372–380.

Scott, H. D., and Smith, M. P., 1973. The aluminum activation log, *The Log Analyst,* 14(5):3–12.

Shipboard Scientific Party, 1990a. Hole 765. *In* Ludden, J. N., Gradstein, F.M., et al., *Proc. ODP, Init. Repts.*, 123: College Station, TX (Ocean Drilling Program), 63–267.

Shipboard Scientific Party, 1990b. Hole 766. *In* Ludden, J. N., Gradstein, F. M., et al., *Proc. ODP, Init. Repts.*, 123: College Station, TX (Ocean Drilling Program), 269–352.

Date of initial receipt: 10 May 1990
Date of acceptance: 29 July 1991
Ms 123B-167

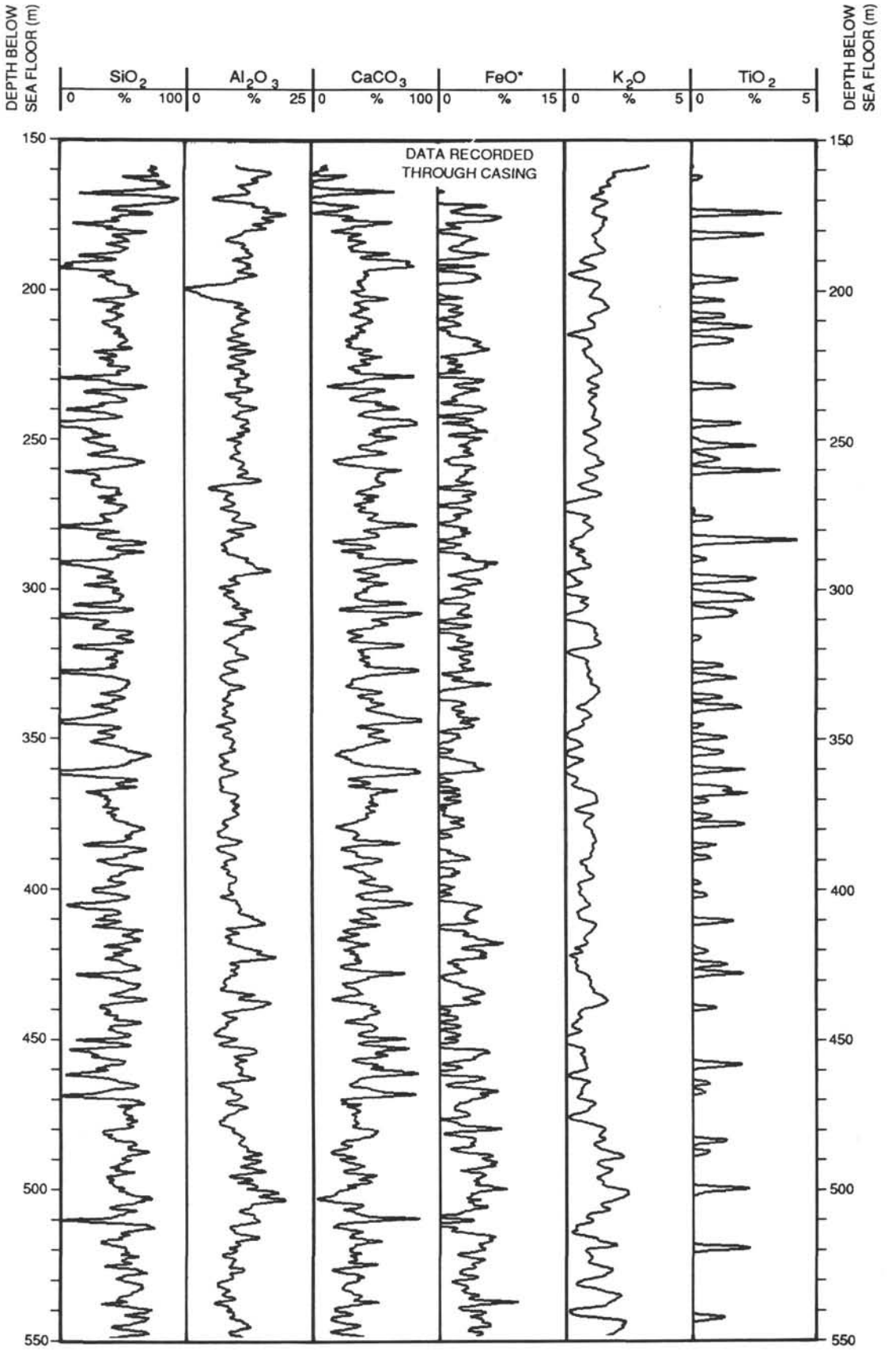

Figure 5. Estimates of major oxides and calcium carbonate from the geochemical logs in the sediment section of Hole 765D.

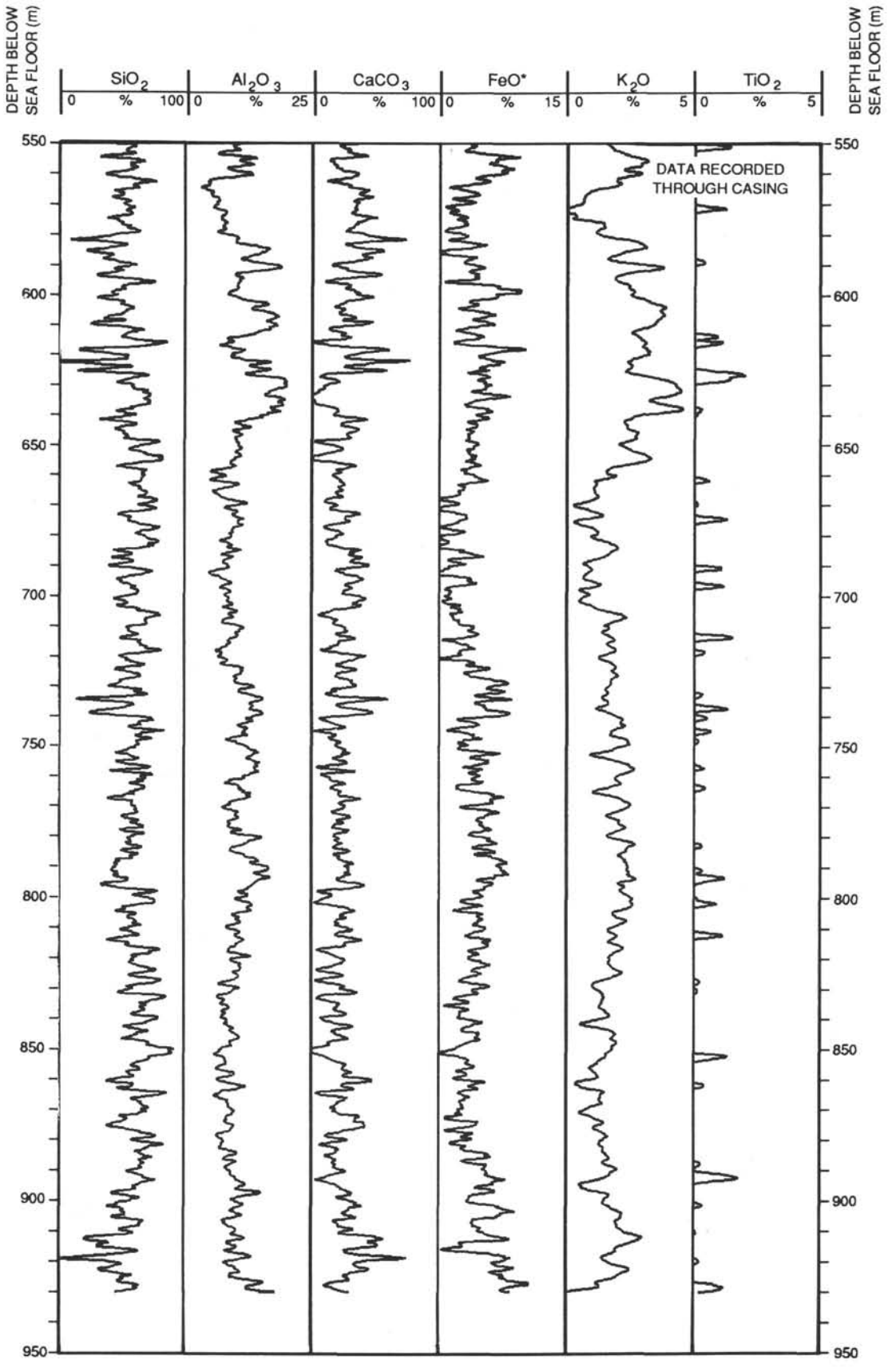

Figure 5 (continued).

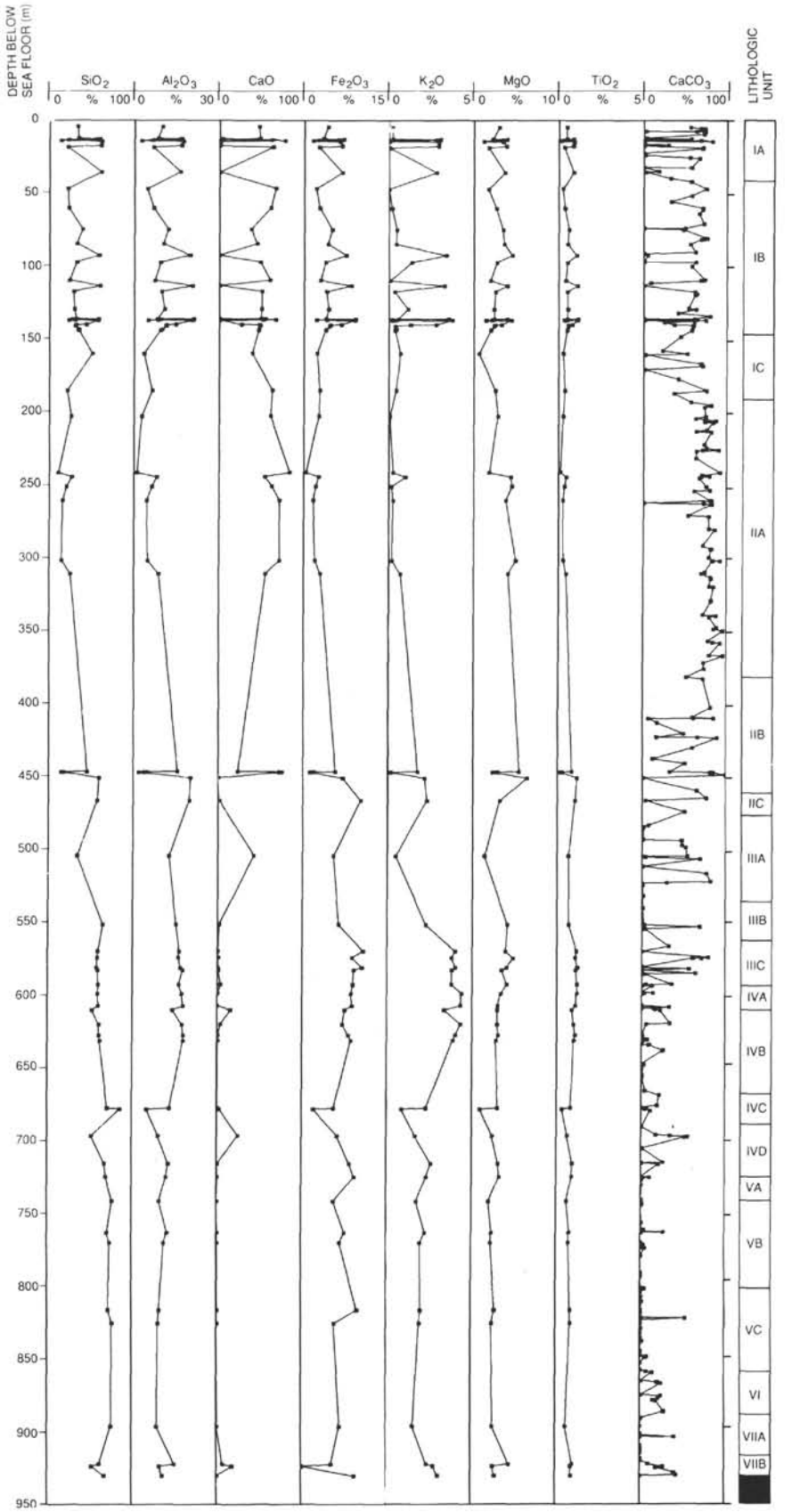

Figure 6. Estimates of major oxides and calcium carbonate from cores in the sedimentary section of Hole 765D. No correction for hole deviation was applied.

[BLANK PAGE]

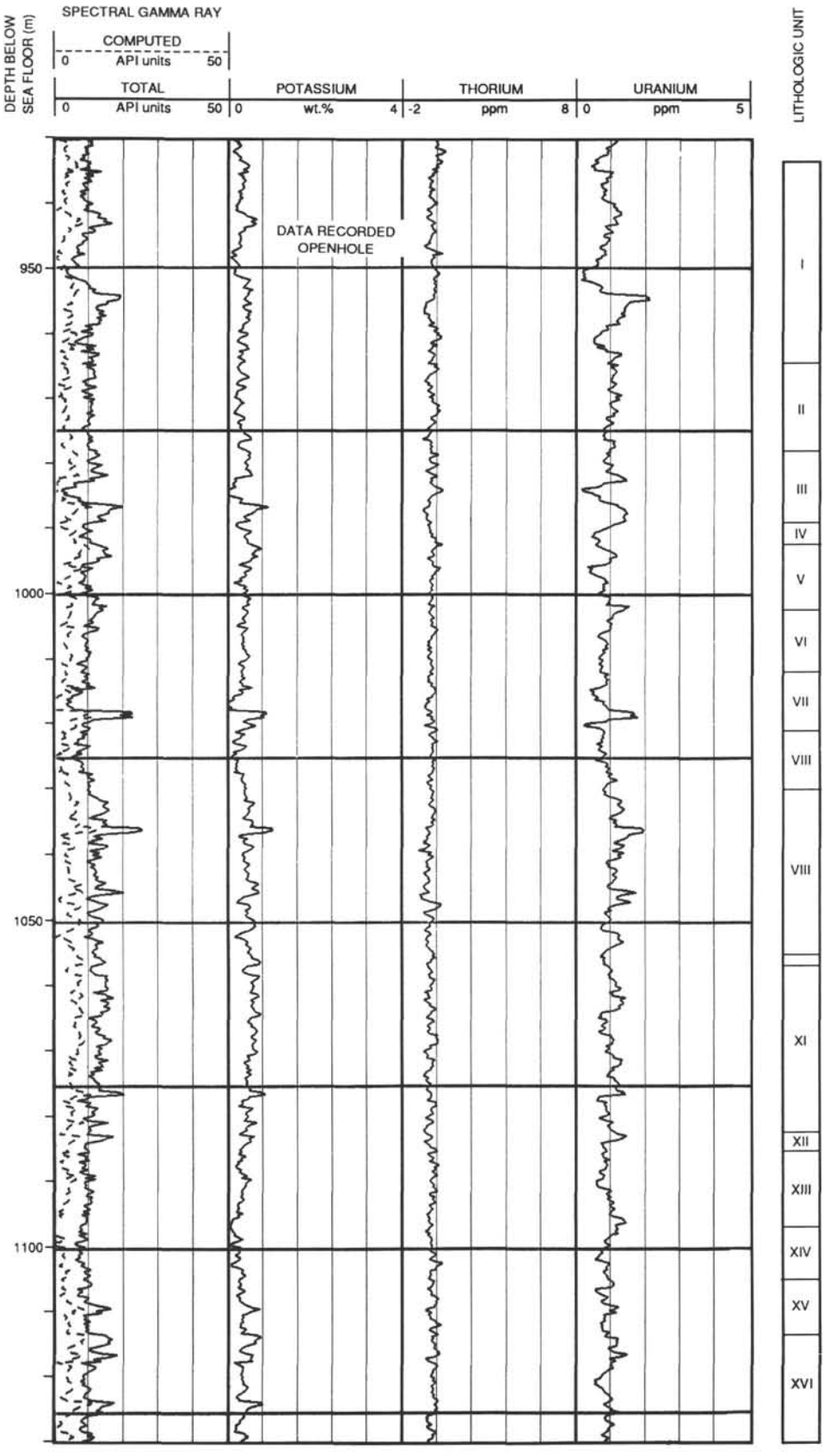

Figure 7. Reprocessed natural gamma-ray data at Hole 765D (basement section).

HOLE 765-D: LEGEND OF LITHOLOGIC UNITS

Basement

Unit I: massive basalt
Unit II: massive basalt
Unit III: massive basalt with pillow basalt and hyaloclastite
Unit IV: pillow basalt with hyaloclastite
Unit V: pillow basalt
Unit VI: massive basalt
Unit VII: diabase
Unit VIII: pillow basalt
Unit X: pillow basalt with hyaloclastite
Unit IX: pillow basalt
Unit XI: pillow basalt with hyaloclastite
Unit XII: pillow basalt
Unit XIII: pillow basalt
Unit XIV: massive basalt
Unit XV: pillow basalt
Unit XVI: pillow basalt

Figure 7 (continued).

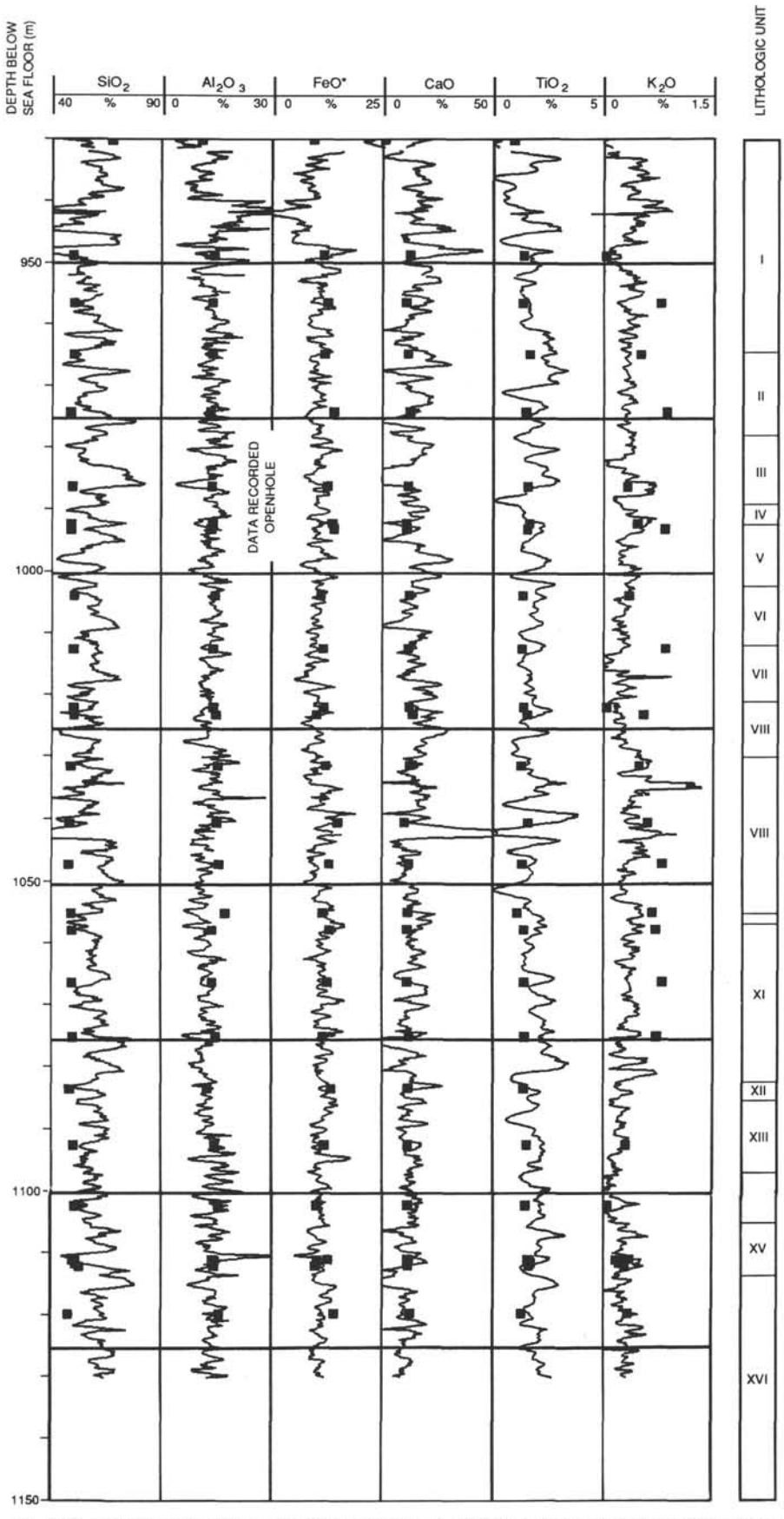

Figure 8. Estimates of major oxides from the geochemical logs in the basement section of Hole 765D.

[BLANK PAGE]

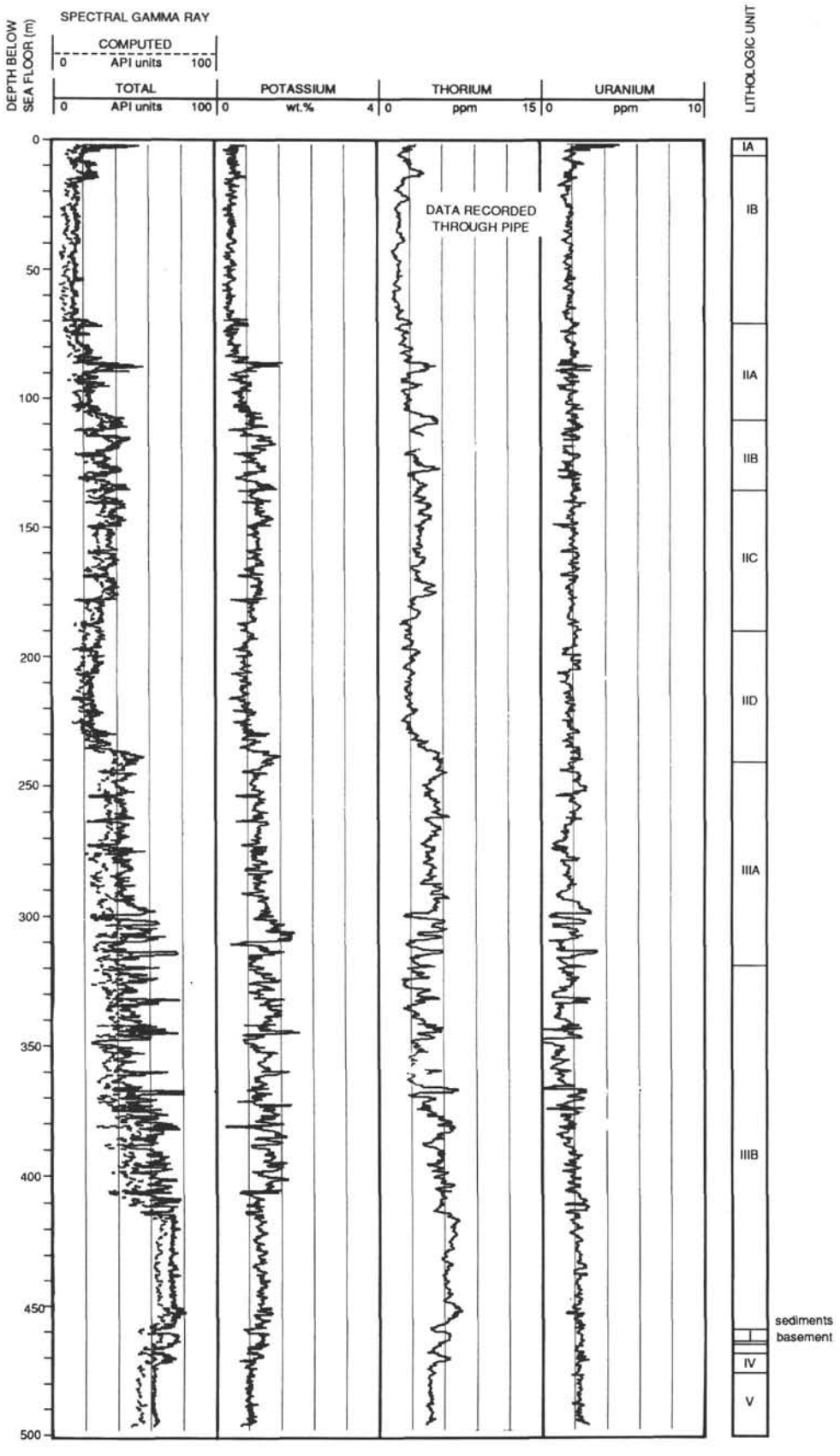

Figure 9. Reprocessed natural gamma-ray data at Hole 766A.

HOLE 766-A: LEGEND OF LITHOLOGIC UNITS

Sediments

Subunit IA: nannofossil ooze with siliceous nannofossils
Subunit IB: nannofossil ooze without siliceous nannofossils
Subunit IIA: nannofossil ooze and plymictic conglomerate
Subunit IIB: calcareous ooze and clay
Subunit IIC: clayey nannofossil ooze and chalk
Subunit IID: nannofossil and calcareous chalk
Subunit IIIA: claystone
Subunit IIIB: sandstone and siltstone

Basement

Unit I: phyric basalt
Unit II: aphyric basalt
Unit III: aphyric basalt
Unit IV: aphyric vesicular basalt
Unit V: aphyric diabase

Figure 9 (continued).

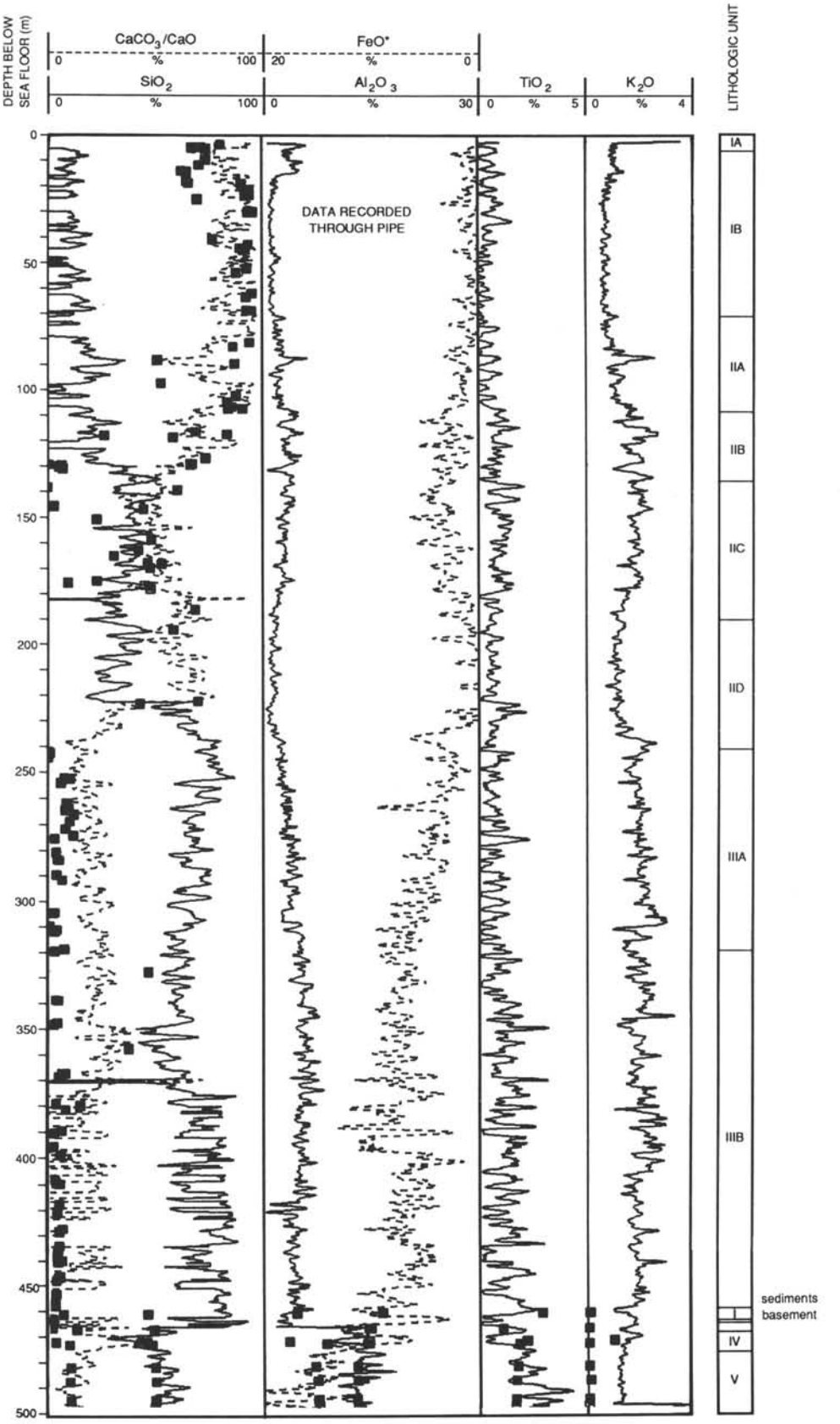

Figure 10. Measurements of major oxides and calcium carbonate from geochemical logs at Hole 766A. $CaCO_3$ and oxide core measurements also are displayed for comparison in the sediment and basement sections, respectively.